

Bulletin of Atmospheric Science and Technology

A network of water vapor Raman lidars for improving heavy precipitation forecasting in southern France – Introducing the WaLiNeAs initiative --Manuscript Draft--

Manuscript Number:	BAST-D-21-00007	
Full Title:	A network of water vapor Raman lidars for improving heavy precipitation forecasting in southern France – Introducing the WaLiNeAs initiative	
Article Type:	Research Article	
Funding Information:	Agence Nationale de la Recherche (ANR-20-CE04-0001)	Dr. Cyrille Flamant
	MISTRALS/HyMeX	Dr. Cyrille Flamant
	Horizon 2020 Framework Programme (654109)	Not applicable
	Horizon 2020 Framework Programme (778349)	Not applicable
	Horizon 2020 Framework Programme (871115)	Not applicable
	Spanish Ministry of Science and Innovation (PID2019-103886RB-I00)	Not applicable
	Spanish Ministry of Economy, Industry and Competitiveness (CGL2017-90884-REDT)	Not applicable
	Agencia Estatal de Investigación (MDM-2016-0600)	Not applicable
Abstract:	<p>Extreme heavy precipitation events (HPEs) pose a threat to human life but remain difficult to predict. Considerable efforts to improve the forecast skills for such severe events have been made in recent years and significant progress has been realized through the development of convection-permitting numerical weather prediction (NWP) systems. However, our ability to predict such high-impact events remains limited because of the lack of adequate high frequency, high resolution water vapor (WV) observations in the low troposphere (below 3 km). Having such information will significantly improve weather forecasting and thus anticipate the floods associated with the HPEs. Indeed, HPEs occurring in small and steep watersheds are responsible for the triggering of flash floods with a sudden and often violent onset and rapid rising time, typically from 1 to 6 h following the causative rainfall.</p> <p>We aim to implement an integrated prediction tool, coupling network measurements of WV profiles and a numerical weather prediction model to precisely estimate the amount, timing and location of rainfall associated with HPEs in southern France (struck by ~7 HPEs per year on average during the fall).</p> <p>The proposed Water vapour Lidar Network Assimilation (WaLiNeAs) project is a unique, innovative initiative that will allow for assimilating high-vertical-resolution lidar-derived WV profiles in the first 3 km of the troposphere in a quasi-operational setting. The benefit of WaLiNeAs to the academic and operational communities is dual: advance knowledge of the complex thermodynamical and dynamical processes controlling the life cycle of HPEs and enhance the predictability of HPEs in southern France at scales relevant for meteorological studies. Increasing the accuracy of forecasts of quantitative precipitation will also help addressing a pressing societal demand.</p> <p>A network of 6 autonomous Raman WV lidars will be deployed around the Western Mediterranean to provide measurements with high vertical resolution and accuracy, closing critical gaps in lower troposphere WV observations by current operational networks and satellites. Near real-time processing and ensemble assimilation of the WV data in the French Application of Research to Operations at Mesoscale (AROME-France) model, using a four-dimensional Ensemble Variational approach with 15 min updates, is expected to enhance the model capability for kilometer-scale prediction of HPEs over southern France up to 48 hours in advance.</p> <p>The field campaign is scheduled to start early September 2022, to cover the period most propitious to heavy precipitation events in southern France. The Raman WV lidar</p>	

	<p>network will be operated by a consortium of French, German, Italian and Spanish research groups. Lidar vertical profiles will be made available to Météo-France shortly after being acquired up to 96 times per day.</p> <p>Besides demonstrating the potential of WV lidar data assimilation in a near real-time quasi-operational context, an ancillary objective of the project is also to show that Raman lidars can be left to operate continuously almost unattended for a period of at least 3 months. It is a prerequisite in the perspective of future deployment of operational Raman lidar systems meant to fulfil the observational gaps in WV in the lower troposphere of the current operational observation networks and satellites. This project will lead to recommendations on the lidar data processing for future operational exploitation in NWP systems.</p>
Corresponding Author:	Cyrille Flamant, PhD Centre National de la Recherche Scientifique Paris, FRANCE
Corresponding Author Secondary Information:	
Corresponding Author's Institution:	Centre National de la Recherche Scientifique
Corresponding Author's Secondary Institution:	
First Author:	Cyrille Flamant, PhD
First Author Secondary Information:	
Order of Authors:	Cyrille Flamant, PhD
	Patrick Chazette, PhD
	Olivier Caumont, PhD
	Paolo Di Girolamo, PhD
	Andreas Behrendt, PhD
	Michaël Sicard, PhD
	Julien Totems
	Diego Lange
	Nadia Fourrié
	Pierre Brousseau
	Clotilde Clotilde Augros
	Alexandre Baron
	Marco Cacciani
	Adolfo Comerón
	Benedetto De Rosa
	Veronique Ducrocq
	Pascal Genau
	Laurent Labatut
	Constantino Muñoz-Porcar
	Alejandro Rodríguez-Gómez
	Donato Summa
	Rohith Thundathil
	Volker Wulfmeyer
Order of Authors Secondary Information:	

Author Comments:	
Suggested Reviewers:	<p data-bbox="579 155 1500 306">Silvio Davolio, PhD Researcher, CNR-ISAC S.Davolio@isac.cnr.it Specialist in modelling of climate and meteorology. Participated to the HyMeX field campaign.</p> <p data-bbox="579 317 1500 438">Tetsu Sakai, PhD Researcher, Meteorological Research Institute tetsu@mri-jma.go.jp Raman lidar for water vapor measurements specialist</p> <p data-bbox="579 449 1500 571">Alex Papyannis, PhD professor, National Technical University of Athens apdlidar@mail.ntua.gr Lidar specialist</p> <p data-bbox="579 581 1500 741">Samiro Khodayar, PhD Researcher, Mediterranean Centre for Environmental Studies khodayar_sam@gva.es Modelling and meteorology, specialist of Mediterranean weather systems, water vapour observations, participated to the HyMeX field campaign</p> <p data-bbox="579 751 1500 873">Marta Janiskova, PhD Senior scientist, ECMWF: European Centre for Medium Range Weather Forecasts marta.janiskova@ecmwf.int numerical weather prediction, water vapour data assimilation</p> <p data-bbox="579 884 1500 1005">Saturo Yoshida, PhD Senior Researcher, Meteorological Research Institute syoshida@mri-jma.go.jp Lidar, Data assimilation, lightning, Remote sensing</p>

A network of water vapor Raman lidars for improving heavy precipitation forecasting in southern France – Introducing the WaLiNeAs initiative

Cyrille Flamant¹, Patrick Chazette², Olivier Caumont³, Paolo Di Girolamo⁴, Andreas Behrendt⁵, Michaël Sicard^{6,7}, Julien Totems², Diego Lange⁵, Nadia Fourrié³, Pierre Brousseau³, Clotilde Augros³, Alexandre Baron², Marco Cacciani⁴, Adolfo Comerón⁶, Benedetto De Rosa⁴, Veronique Ducrocq³, Pascal Genau¹, Laurent Labatut³, Constantino Muñoz-Porcar⁶, Alejandro Rodríguez-Gómez⁶, Donato Summa^{4,8}, Rohith Thundathil⁵ and Volker Wulfmeyer⁵

¹LATMOS/IPSL, CNRS-SU-UVSQ, Sorbonne Université, Paris, France

²LSCE/IPSL, CNRS-CEA-UVSQ, University Paris-Saclay, CEA Saclay, Gif sur Yvette, France

³CNRM, Université de Toulouse, Météo-France, CNRS, Toulouse, France

⁴Scuola di Ingegneria, Università della Basilicata, Potenza, Italy

⁵Universität Hohenheim, Institut für Physik und Meteorologie, Stuttgart, Germany

⁶CommSensLab, Department of Signal Theory and Communications, Universitat Politècnica de Catalunya (UPC), 08034 Barcelona, Spain

⁷Ciències i Tecnologies de l'Espai-Centre de Recerca de l'Aeronàutica i de l'Espai, Institut d'Estudis Espacials de Catalunya (CTE-CRAE/IEEC), Universitat Politècnica de Catalunya (UPC), 08034 Barcelona, Spain

⁸CNR-IMAA, Tito Scalo center, Potenza, Italy

Abstract

Extreme heavy precipitation events (HPEs) pose a threat to human life but remain difficult to predict. Considerable efforts to improve the forecast skills for such severe events have been made in recent years and significant progress has been realized through the development of convection-permitting numerical weather prediction (NWP) systems. However, our ability to predict such high-impact events remains limited because of the lack of adequate high frequency, high resolution water vapor (WV) observations in the low troposphere (below 3 km). Having such information will significantly improve weather forecasting and thus anticipate the floods associated with the HPEs. Indeed, HPEs occurring in small and steep watersheds are responsible for the triggering of flash floods with a sudden and often violent onset and rapid rising time, typically from 1 to 6 h following the causative rainfall.

We aim to implement an integrated prediction tool, coupling network measurements of WV profiles and a numerical weather prediction model to precisely estimate the amount, timing and location of rainfall associated with HPEs in southern France (struck by ~7 HPEs per year on average during the fall).

The proposed Water vapour Lidar Network Assimilation (WaLiNeAs) project is a unique, innovative initiative that will allow for assimilating high-vertical-resolution lidar-derived WV profiles in the first 3 km of the troposphere in a quasi-operational setting. The benefit of WaLiNeAs to the academic and operational communities is dual: advance knowledge of the complex thermodynamical and dynamical

40 processes controlling the life cycle of HPEs and enhance the predictability of HPEs in southern France
41 at scales relevant for meteorological studies. Increasing the accuracy of forecasts of quantitative
42 precipitation will also help addressing a pressing societal demand.

43 A network of 6 autonomous Raman WV lidars will be deployed around the Western Mediterranean to
44 provide measurements with high vertical resolution and accuracy, closing critical gaps in lower
45 troposphere WV observations by current operational networks and satellites. Near real-time
46 processing and ensemble assimilation of the WV data in the French Application of Research to
47 Operations at Mesoscale (AROME-France) model, using a four-dimensional Ensemble Variational
48 approach with 15 min updates, is expected to enhance the model capability for kilometer-scale
49 prediction of HPEs over southern France up to 48 hours in advance.

50 The field campaign is scheduled to start early September 2022, to cover the period most propitious to
51 heavy precipitation events in southern France. The Raman WV lidar network will be operated by a
52 consortium of French, German, Italian and Spanish research groups. Lidar vertical profiles will be made
53 available to Météo-France shortly after being acquired up to 96 times per day.

54 Besides demonstrating the potential of WV lidar data assimilation in a near real-time quasi-operational
55 context, an ancillary objective of the project is also to show that Raman lidars can be left to operate
56 continuously almost unattended for a period of at least 3 months. It is a prerequisite in the perspective
57 of future deployment of operational Raman lidar systems meant to fulfil the observational gaps in WV
58 in the lower troposphere of the current operational observation networks and satellites. This project
59 will lead to recommendations on the lidar data processing for future operational exploitation in NWP
60 systems.

61 Introduction

62
63 Heavy precipitation events (HPEs) pose a threat to human lives (e.g., Llasat et al. 2013) as well as the
64 economy and the environment of impacted regions. HPEs occurring in small and steep watersheds are
65 responsible for the triggering of flash floods with a sudden and often violent onset and rapid rise of
66 rivers, typically from 1 to 6 h following the causative rainfall (Gaume et al., 2009). Flash floods and
67 landslides lead to fatalities, loss of crops and livestock, damage to infrastructures, as well as disruption
68 of transport and communication. HPEs remain difficult to predict. Considerable efforts to improve the
69 forecast skill for such severe events have been made in recent years and significant progress has been
70 realized through the development of kilometer-scale numerical weather NWP systems (Ducrocq et al.,
71 2014) and data assimilation techniques (e.g. Kwon et al., 2018, Gustafsson et al., 2018). However, our
72 ability to predict such high-impact events remains limited because of the lack of adequate high

73 frequency, high resolution vertically resolved water vapor (WV) observations in the low troposphere
74 to be assimilated in NWP systems, and especially in the boundary layer (Weckwerth et al., 2004;
75 Wulfmeyer et al., 2015; Leuenberger et al., 2020).

76
77 The implementation of an integrated prediction tool, coupling network measurements of WV profiles
78 and a NWP model, to precisely estimate the amount, timing, and locations of rainfall associated with
79 HPEs up to 48 hours in advance, is a strong societal demand, especially in regions of France most
80 exposed to heavy rainfall (defined as maximum accumulation in excess of 150 mm per day, Ricard et
81 al., 2012) as those located along the Mediterranean coast. Figure 1 shows the geographical distribution
82 of HPEs obtained from raingauges for the period 1970-2019) in Southern France. Over this period, HPEs
83 are most numerous in Languedoc-Roussillon, along the southern edge of the Cevennes range, between
84 the Mediterranean coastline and the southern Alps, and along the eastern side of Corsica. The two
85 most important HPEs seen in Figure 1 are located in the Aude department and are related to the 12–
86 13 November 1999 event (Nuissier et al., 2008; Ducrocq et al., 2008) and the 14-15 October 2018 event
87 (Caumont et al., 2020). Large amounts of rainfall associated with these cases were attributed to strong
88 synoptic forcing and associated with a quasi-stationary mesoscale convective systems (MCSs) which,
89 for instance, led to accumulated surface precipitation reaching about 620 mm for the former event
90 Ducrocq et al. (2008). Other remarkable events in the same area (Languedoc-Roussillon and Cevennes)
91 are seen in the Hérault and Gard departments which are also linked to catastrophic events such as the
92 13-14 October 1995 and 8-9 September 2002 cases, respectively (Ducrocq et al., 2008) also related to
93 torrential rainfall cause by stationary MCSs. In the southern Alps area, remarkable HPE cases include
94 the Vaison-La-Romaine event in the Vaucluse department (22 September 1992) and the Côte d’Azur
95 event in the Alpes Maritimes department (3 October 2015). In addition, two other cases are included
96 that have been identified during the hydrological Cycle in the Mediterranean Experiment First Special
97 Observing Period (HyMeX SOP1) on 14 and 26 October and 2012 (Duffourg et al., 2016, 2018). Finally,
98 a famous HPE in Corsica was the 31 October-1 November 1993 case which affected the eastern side of
99 Island with up to 450 mm of rain in a day in several locations.

100
101 Southern France is a region stricken by an average of 7 HPEs per year during the fall (September to
102 November) (Ricard et al., 2012, Ducrocq et al., 2014) as illustrated by Figure 2 for the period 1970-
103 2019. It is worth noting that HPEs can also occur outside of the September-November period, as for
104 instance in December when more than an event per year can be observed. All other months exhibit
105 less that one HPE per year, with the minimum in the monthly climatology being observed in June and
106 July, which are the months less favorable for sustainability of HPEs (lower sea surface temperatures
107 than in the fall and less eastward moving low pressure disturbances across the Mediterranean).

108 Furthermore, and in close connection with climate change issues, the analysis of extreme
109 Mediterranean rainfall events for the French regions over the last few decades shows an intensification
110 of heavy rainfall between 1961 and 2015 (+22% on the annual maximum daily totals) and an increase
111 in the frequency of the strongest Mediterranean episodes, particularly those exceeding the 200 mm
112 threshold in 24 hours (Ribes et al., 2019).

113
114 Accurate characterization of WV in the lower atmosphere is essential for quantitative precipitation
115 forecasting associated with HPEs (e.g. Behrendt et al., 2011 and references therein). However, the
116 spatial and temporal variability of the WV field is very high, notably due to the fact that (i) the WV field
117 (unlike the temperature field) is not subject to mass adjustment processes and (ii) water coexists in
118 three phases in the atmosphere. Furthermore, WV is an essential atmospheric meteorological and
119 climatological variable but one that is still difficult to measure, as WV concentrations can vary by three
120 orders of magnitude in the troposphere (typically from 10 g kg^{-1} near the surface to 0.01 g kg^{-1} in the
121 upper troposphere).

122
123 Despite the undeniable contribution of microwave and infrared sounders, the assimilation of
124 atmospheric WV-related observations from space still suffers from many limitations: (i) insufficient
125 vertical resolution and accuracy below 3 km to describe precisely the very strong gradients of the
126 moisture profiles observed in the lower troposphere (Chazette et al., 2014; Wulfmeyer et al., 2015),
127 i.e. in a region key to understand convective initiation and the life cycle of heavy precipitating systems,
128 and (ii) poor temporal sampling due to the fact that infrared and microwave sounders are embarked
129 on meteorological satellites and cannot fully grasp the strong temporal variability of the WV field.
130 Global Navigation Satellite System radio-occultation (GNSS RO) are observations from satellite
131 providing information on humidity at high vertical resolution ($\sim 100 \text{ m}$) down to 1 km above the Earth
132 surface through the limb sounding. However, they suffer from 3 major drawbacks that currently limit
133 their interest for data assimilation in the French limited area operational Application of Research to
134 Operations at MEscale (AROME-France) model. First, the horizontal resolution of GNSS RO products
135 is too coarse in the troposphere (a few hundred km, as they consist of path-integrated measurements)
136 which is not appropriate for a fine scale NWP system (e.g. AROME-France has a 1.3 km grid size, and
137 90 vertical levels between the surface and 10 hPa, 33 of which are below 2000 m). Second, GNSS RO
138 observations do not allow to observe the WV in the first kilometer of the atmosphere which is of great
139 importance for monitoring moisture upstream of HPE hotspots. Third, there are very few GNSS RO
140 observations available in each AROME-France 1-hour assimilation window. For instance, the WV
141 products currently assimilated from the plethora of microwave and infrared sensors on polar orbiting
142 spacecraft only represent 15% of the data ingested in the AROME-France operational model. In

143 conclusion, currently available GNSS RO products are not suitable for improving HPE forecast through
144 data assimilation.

145
146 Currently, 85% of the WV products assimilated in AROME-France come from surface stations, radar
147 reflectivity near surface, aircraft, surface-based GNSS and radiosoundings. However, only the latter
148 can provide vertically resolved WV profiles above the surface, and this twice a day at best. Ground-
149 based GNSS networks only provide integrated WV contents whereas radars just provide indirect
150 information on WV in precipitating systems. Surface stations only provide information on moisture
151 very close to the surface and aircraft are currently very poorly equipped with moisture sensors.

152
153 Much of the AROME-France domain covers the western Mediterranean which is usually upstream of
154 convective systems (Figure 3), while observation systems used for assimilation (radar, GNSS, SYNOP
155 stations) are primarily terrestrial. This is a major caveat because this is where the fast-evolving
156 evaporation and air mass moistening processes take place that are crucial to understand and anticipate
157 the development of HPEs downstream over southern France. This explains why HPEs in Southern
158 France are quite challenging to forecast with sufficient lead-time compatible with hazard warnings.
159 Hence, the assimilation of data in the lower layers across the Western Mediterranean and available in
160 near real-time will benefit prediction of HPEs at the mesoscale.

161 The project WaLiNeAs (Water vapor Lidar Network Assimilation) aims at bringing together French,
162 Italian, German and Spanish scientists concerned with improving HPEs forecasts around the
163 Mediterranean. The members of the international consortium have joined forces to tackle the issues
164 and challenges highlighted above. This paper describes the rationale of the WaLiNeAs initiative as well
165 as the measurement and assimilation strategies central to project. It also highlights the key
166 expectations from the programme funded by several agencies in France, Italy, Germany and Spain.

167 168 Challenges, Objectives and Strategy

169
170 In the framework of the WaLiNeAs initiative, we aim to implement such an integrated prediction tool
171 to enhance the forecast of HPEs in southern France. A consortium of French, German, Italian and
172 Spanish research groups will deploy a network of 6 autonomous WV lidars for providing measurements
173 with high vertical resolution and accuracy across the Western Mediterranean in fall 2022, closing
174 critical gaps in lower troposphere WV observations by current operational networks and satellites. The
175 proposed WV lidar network has been designed to account for all relevant WV sources and transport
176 patterns known to contribute to the generation of HPEs in Southern France. This network will aim at
177 demonstrating the benefit of the assimilation of vertically resolved WV data in the forthcoming version
178 of the operational 1.3 km grid size AROME-France NWP system (Brousseau et al., 2016; Montmerle et

179 al., 2018) which enables ensemble-variational data assimilation for kilometer-scale prediction of heavy
180 precipitation over Southeastern France (Desroziers et al, 2014). The ensemble-variational data
181 assimilation system that will be available in 2022 will produce hourly analyses and will be operated
182 with a rapid update cycle of assimilation of new observations at least each 15 min.

183
184 The WaLiNeAs project is a unique, innovative initiative that will allow for assimilating lidar-derived WV
185 profiles in the lower troposphere with hectometer-scale vertical resolution in near-real time conditions
186 for a continuous period of at least 3 consecutive months. The benefit of WaLiNeAs to the academic
187 and operational communities is dual: advance knowledge of the processes at play in the life cycle of
188 HPEs and enhance the predictability of HPEs in Southern France at scales relevant for meteorological
189 studies. Both aspects are dealt with in the framework of WaLiNeAs.

190
191 Finally, the breakthrough science that will be carried out in the framework of WaLiNeAs concerns:

- 192 ○ characterizing the predictability of HPEs and uncertainties in the prediction of the position,
193 evolution and the rainfall amount of the precipitating systems.
- 194 ○ assessing the role of water vapor distribution over the western Mediterranean on the
195 characteristics of the moist inflow (origin, evolution, pathways) feeding deep convection leading
196 to HPEs,
- 197 ○ investigating the role of Mediterranean cyclone in the water cycle and HPEs in the Western
198 Mediterranean,
- 199 ○ understanding the impact of elevated tropical moist plumes on the life cycle of deep convection
200 and related HPEs,
- 201 ○ advancing knowledge on the role of dry intrusions on HPE in cases of frontal precipitation,

202
203 The Raman lidar-derived WV data acquired in the framework of the WaLiNeAs project will be made
204 available to Météo-France shortly after being acquired and will be assimilated up to 96 times per day.

205 The focus of the project will be on providing high quality lidar-derived WV data in the first 3 km of the
206 atmosphere, where no other observational technique can provide adequate data. To that respect, the
207 two most cutting edge aspects of the project are: (i) the near-real time processing and qualification of
208 the lidar data (with WV profiles in the lower troposphere available every 15 min.) and (ii) the proposed
209 system (four-dimensional Ensemble Variational – 4DEnVar (Desroziers et al., 2014)– with kilometeric
210 resolution) for the assimilation of qualified lidar data acquired in the lower troposphere, day and night.

211
212 Besides demonstrating the potential of WV lidar data assimilation in the AROME-France system, an
213 ancillary objective of the project is also to show that Raman lidars can be left to operate continuously
214 almost unattended for a period of at least 3 months. It is a prerequisite in the perspective of
215 future/further deployment of operational Raman lidar systems meant to fulfil the observational gaps

216 in water vapor in the lower troposphere of the current operational observation networks and
217 satellites. This project can be considered as a test bed for the concept of operational use of Raman
218 lidars to be assimilated in a kilometer-scale NWP system.

219
220 The WaLiNeAs project builds on previous experience of the consortium partners, namely:

- 221 ○ Wulfmeyer et al. (2006) have assimilated airborne WV lidar observations acquired during a case
222 study of the International H₂O project (IHOP) with the MM5 mesoscale NWP system and its four-
223 dimensional variational (4D-Var) assimilation system,
- 224 ○ Grzeschik et al. (2008) extended the previous work to the assimilation of the WV observations
225 provided by a ground-based network of Raman lidar systems,
- 226 ○ Bielli et al. (2012) used a pre-operational version of the Météo-France AROME-France NWP system
227 (Seity et al., 2011) and its associated 3D-Var high-resolution assimilation system to evaluate the
228 impact on the quantitative precipitation forecasts of the Convective and Orographically-driven
229 Precipitation Study (COPS) airborne lidar observations collected during July 2007. A continuous
230 assimilation cycle updated every 3 h was run over a month to provide the initial conditions of a
231 sequence of 30 h forecasts carried out over 19 consecutive days,
- 232 ○ an ambitious effort has been conducted to assimilate water vapour mixing ratio observations from
233 the airborne lidar LEANDRE 2 (Lidar Embarqué pour l'étude des Aérosols, des Nuages, de la
234 Dynamique, du Rayonnement et des Espèces minoritaires, developed at LATMOS, Guyancourt,
235 France) and the two ground-based Raman lidars located in Menorca (the Weather Atmospheric
236 Lidar –WALI- developed by LSCE, Gif-sur-Yvette, France) and Candillargues (the BASILicata Lidar –
237 BASIL- developed by the University de la Basilicata, Potenza, Italy) as part of the reanalysis project
238 aiming at assimilating the research observations collected during the HyMeX SOP1 (Richard et al.,
239 2014; Fourrié et al., 2015, 2019, 2021). One month of ground-based Raman lidar data and airborne
240 lidar observations from approximately 20 flights were used in the reanalyses conducted by Fourrié
241 et al. (2015, 2019, 2021),
- 242 ○ Thundathil et al. (2020) assimilated even both water vapour and temperature lidar data into the
243 Weather and Research Forecast model on the convection-permitting scale applying a 3DVAR rapid
244 update cycle and found that especially the assimilation of moisture results in a significant
245 improvement of the model fields.

246
247 All these studies have shown encouraging results in terms of the impact of lidar-derived WV data
248 assimilation on quantitative precipitation forecasts. However, they are based on a limited number of
249 cases, date from a limited number of lidar systems (2 at most) and too short assimilation periods to
250 allow for general conclusions to be drawn in a statistical sense regarding the impact of WV lidar
251 observation assimilation on the quantitative precipitation forecast.

Implementation of WaLiNeAs

As part of the WaLiNeAs initiative, the WV Raman lidars will be operated continuously during 3 months starting early September 2022, to cover the period most propitious to HPEs in southern France (see Figures 1 and 2). The duration of the operation is imposed by the necessity to have a long enough record in order for the WV profiles assimilated to have a significant impact on the moisture fields in the model forecasts. This long dataset is crucial to assess statistical errors and to genuinely evaluate the benefit of Raman lidar water vapor data assimilation for operational NWPS.

This proposal accounts for the fact that Raman lidar technology has reached the level of maturity needed for unattended, continuous operation. Since more than 10 years, automated Raman lidar systems are operated in automatic mode at several observatories and research institutions (Goldsmith et al., 1998; Balin et al., 2004; Reichardt et al., 2021; Dineev et al., 2013; Brocard et al., 2013; Leuenberger et al., 2020). Recently, also mobile systems became available which can be moved for field experiments: This is attested by the large datasets acquired by WALI and BASIL in the field during HyMeX SOP1 (Chazette et al., 2016; Di Girolamo et al., 2020), or by the automated Raman lidar ARTHUS (Atmospheric Raman Temperature and Humidity Sounder, Lange et al., 2019) of University of Hohenheim that operated from a ship for over a month during the EUREC⁴A campaign (Stevens et al., 2021). Figure 3 shows examples of time-height cross-sections of WV mixing ratio measured with WALI from 17 September to 28 October 2012 over Menorca, Spain (Figure 3a), with BASIL over the 12-day time period from 0000 UTC on 17 October 2012 to 0000 UTC on 27 October 2012 over Candillargues, France (Figure 3b), and with ARTHUS between 11 and 19 February 2020 on-board the research vessel Maria S. Merian over the Tropical Atlantic Ocean during the EUREC⁴A campaign (Figure 3c). During HyMeX, WALI acquired 1000 hours of WV mixing ratio profiles while being operated continuously during SOP1 and BASIL acquired over 600 hours of data during the same period, but was operated continuously for 3 days at a time, at most. During EUREC⁴A, ARTHUS collected useful data between 24 January and 19 February 2020, for approximately 620 hours.

We aim to operate a dedicated network of 6 autonomous Raman WV lidars over the Western Mediterranean in locations shown in Figure 4 to monitor the low-level and elevated moisture towards regions most likely to be hampered by HPEs in southern France in the fall as illustrated by Figure 5, and also discussed by Ricard et al. (2012, see their Figure 1), namely: Languedoc-Roussillon (LR), Cévennes-Vivarais (CV), southern Alps (SA) and Corsica (CO). Five of the six Raman lidar systems will be deployed specifically for WaLiNeAs. The 6th system is operating as a fixed, long-term monitoring station. The low-level moisture pathways are inspired by the composite analysis for 40 HPEs made by Ricard et al.

288 (2012), for each of the target areas based on 700–1000-hPa integrated moisture flux and 925-hPa wind
289 speed (see their Figure 11). We are considering sites such as Barcelona and the islands of Menorca in
290 Spain (to monitor the southerly flow upwind of LR, CV and SA, as well as elevated plumes from tropical
291 Africa), Ajaccio in Corsica (to monitor the southerly flow upwind of CO and the easterly flow upwind
292 of LR), Narbonne in the Aude Valley (to monitor the westerly flow from the Atlantic Ocean as well as
293 event over LR), Cannes (to monitor the easterly flow upwind LR and SA) and Montpellier (to monitor
294 the southerly flow and boundary layer upstream of CV). The main moisture patterns leading to HPE in
295 southern France shown in Figure 5 are also based on prior knowledge (Duffourg and Ducrocq, 2013)
296 and on the most recent work conducted on HyMeX SOP1, e.g. Chazette et al. (2016b), Di Girolamo et
297 al. (2016), Duffourg et al. (2018), Khodayar et al., (2018), among others. In an Observing System
298 Simulation Experiment context, Yoshida et al. (2020) have shown that assimilating Raman lidar water
299 vapour data on the windward side of heavy precipitation was likely to improve precipitation forecasts.

300
301 The worth of installing a Raman lidar system to monitor WV upstream of HPE-prone target area further
302 is illustrated in Figure 6. In Figure 6a, we show the density distribution of all WV vertical profiles
303 acquired with the WALI system installed in the city of La Ciutadella, in Menorca, during the entire
304 HyMeX SOP1 (see Figure 4 for the location of La Ciutadella). WALI was operating upstream of target
305 areas in Southern France, namely LR, CV and SA. The distribution highlights the spread in WV mixing
306 ratio observed upstream of the Western Mediterranean coastline (color) around the mean profiles
307 (black solid line). Figure 6a stresses out that in the course of the HyMeX SOP1, the highest occurrence
308 of WV was found below 2 km amsl (where WV mixing ratio in on average comprised between 5 and 15
309 g kg^{-1}) and above 5 km amsl (where values are very low, less than 1.5 g kg^{-1}). The spread below 2 km
310 amsl reaches 6 g kg^{-1} for WV mixing ratio values occurring more than 30 %, and more than doubles for
311 WV mixing ratio values occurring more than 10% of the time. Figure 6b and 6c show the density
312 distribution of WV mixing ratio in HPE-free conditions and in HPE conditions, respectively, for two 5-
313 day periods. The HPE-free period selected is from 2 to 6 October 2012, during which no HPEs were
314 observed in the Western Mediterranean basin. For the HPE conditions, we selected the period from 7
315 to 11 October 2012, up to 4 days ahead of HPE events observed in the CV, namely IOP12a on 11-12
316 October (Khodayar et al., 2018) and IOP 13 on 14-16 October (Duffourg et al., 2018). Above 2 km amsl,
317 the WV mixing ratio distribution for the no-HPE period (Figure 6b) is skewed towards small values than
318 in the HPE period (Figure 6c) up to 8 km amsl. the average WV mixing ratio profile, computed as the
319 barycenters of the distributions at each altitude bin (pink and red solid lines, for the HPE-free and HPE
320 periods, respectively), overlain in Figure 6b and 6c, are also shown in Figure 6d. They highlight that,
321 between 0.75 and 8 km amsl, the troposphere is significantly moister in HPE conditions than in HPE-
322 free conditions. The marine boundary layer is also slightly more moist in HPE conditions below 300 m

323 amsl. The integrated water vapour content profile, computed at the integral of the lidar-derived
324 specific humidity profiles from the ground upward, in HPE-free conditions (pink solid line) and in HPE
325 conditions (red solid line) is shown in Figure 6e. Over the depth of the lower troposphere, i.e. below 8
326 km amsl, the difference between HPE and HPE-free conditions reaches 10 kg m^{-2} . The integrated water
327 vapour content in HPE conditions ($\sim 33 \text{ kg m}^{-2}$) are comparable to those derived from global positioning
328 system by Khodayar et al. (2018) during IOP 12, even though slightly smaller due to the fact that we
329 are only considering partial columns. The above analysis clearly suggests that Raman lidar-derived WV
330 mixing ratio profiles collected in Menorca in a period up to 4 days ahead of HPEs in the CV area are
331 significantly moister than for a 4-day period when no HPE events are observed in Southern France,
332 thereby providing data worthy of assimilation in a HPE forecasting context.

333
334 The 5 mobile Raman lidar systems that will be operating in the field are rugged and transportable
335 systems that have operated in many locations in recent years:

- 336 ○ The Weather Atmospheric Lidar (WALI, Chazette et al., 2014) developed at LSCE, which was
337 involved in the SOP1 of HyMeX (Chazette et al., 2016a,b; Di Girolamo et al., 2020) or during the
338 Pollution in the ARctic System (PARCS) project (Totems et al., 2019) and recently during the
339 Lacustrine-Water vApor Isotope inVentory Experiment (L-WAIVE) project (Chazette et al., 2020),
- 340 ○ The Airborne Lidar for Atmospheric Studies (ALIAS, Chazette et al., 2012; Chazette et al., 2020)
341 developed at LSCE,
- 342 ○ The Lidar for Automatic Atmospheric Surveys using Raman Scattering (LAASURS; Chazette et al.,
343 2017, 2019, 2020) developed at LSCE,
- 344 ○ The University of BASILicata ground-based Raman Lidar system (BASIL), which was involved in
345 HyMeX (Di Girolamo et al., 2009, 2016, 2017, 2020; Stelitano et al., 2019),
- 346 ○ The Atmospheric Raman Temperature and Humidity Sounder (ARTHUS, Lange et al., 2019) of the
347 University of Hohenheim.

348
349 The fixed Raman lidar system that will operate in Barcelona is the lidar system of Universitat Politècnica
350 de Catalunya (UPC, Muñoz-Porcar et al. 2018, 2021) which is in operation since 1993 and is part of the
351 European Aerosol Research Lidar Network (EARLINET) since 2000 and of the European Research
352 Infrastructure for the observation of Aerosol, Clouds, and Trace Gases (ACTRIS) since 2011.

353
354 For details on the instruments (emission unit, reception unit, spatio-temporal sampling strategy, etc.),
355 the reader is referred to the existing body of literature listed above and are summarized in Table 1.
356 LAASURS and ALIAS will be upgraded to WV Raman lidar prior to the start of the fall 2022 field
357 campaign.

358

1 359 The lidar data will be collected, disseminated, and monitored in real time, as would be done in an
2
3 360 operational context. Since it is unrealistic to set up a full real-time operational NWP system dedicated
4
5 361 to a single observing system (the cost of real-time high-performance computing with human
6
7 362 supervision far exceeds funds allotted to WaLiNeAs), the lidar data assimilation will be evaluated in a
8
9 363 quasi-operational environment, i.e., with the same tools and data, but without the associated
10
11 364 resources necessary for real-time operations. This framework will allow deriving results that will hold
12
13 365 true for an operational context, at an economic cost.
14
15 366

16 367 Project organisation and structure 17 368 18 369

19 370 The project is organized around 4 scientific tasks aimed at developing an innovative integrated
20
21 371 forecasting tool in order to pave the way towards an operational, breakthrough HPE-related hazard
22
23 372 warning capability for southern France and Corsica as well as work on the cutting-edge science linked
24
25 373 with the development of such an innovative tool.

26 374 **WP1 (field campaign)** will drive the necessary experimental/instrumental deployments to achieve the
27
28 375 acquisition of WV profiles and the near-real time transmission of the data to the French Weather
29
30 376 Service. This will include the upgrade of the Raman lidar systems to be deployed, as well as the
31
32 377 definition of the exact location of the implementation sites and complementary instruments, the data
33
34 378 transmission protocols and data quality assurance as well as the characterization of system calibration.
35
36 379 WP1 is organized around 3 main activities:

37 381 38 382 ➤ *Upgrade and preparation of lidar systems* 39 383

40 384 The WV-Raman upgrades consist in adding a H₂O-Raman channel on each lidar and the development
41
42 385 of an acquisition chain. The lasers will be upgraded in energy to improve the signal to noise ratio. This
43
44 386 will ensure that the output energy of the systems as well as their performances (precision, systematic
45
46 387 error on WV profiles, etc...) will be same as the operational WALI system. Note that these two mini-
47
48 388 lidar systems will be autonomous and connected via Internet. Prior to the field campaign, a thorough
49
50 389 intercomparison of WV profiles between the operational WALI Raman lidar and the upgraded Raman
51
52 390 systems (LAASURS and ALIAS) will be undertaken.
53 391

54 392 ➤ *Real time data processing and data transmission* 55 393

56 394 For real-time purpose, the six Raman lidars will deliver 2-4 times an hour profiles which are averaged
57
58 395 over 15 minutes with vertical resolution of 100 m and a targeted root-mean-square-error of 0.4 g kg⁻¹
59
60 396 in the first 3 km, day and night. Performances are expected to exceed these target values during the
61
62
63
64
65

397 night for all systems (WALI, ALIAS, LAASURS, BASIL, ARTHUS and UPC/EARLINET). In addition to the
1 398 water vapor mixing ratio profiles, the statistical uncertainties of these profiles as well as the
2
3 399 atmospheric variance determined with the auto-covariance technique (Lenschow et al., 2000) will be
4
5 400 provided. It is a significant advantage of the lidar technique that also these error profiles can be
6
7 401 determined and consequently be used for the data assimilation.

8 402
9 403
10 404 The WV profile acquisition, processing and transmission sequence is anticipated to span over 25
11
12 405 minutes (Figure 7). For the analysis at XXXX UTC, the assimilation system will ingest observations made
13
14 406 between XXXX UTC - 30 min and XXXX UTC + 30 min. Every 15 min between XXXX UTC - 30 min and
15
16 407 XXXX UTC + 30 min, the WV lidar data (resulting from a 15 min. average) will be processed and errors
17
18 408 calculated within a 5 min window, and then transmitted in an additional 5 min window (Figure 7).
19
20 409 There will be some overlap in the processing of each profile: as soon as the 15 min measurement
21
22 410 period (in green in Figure 7) is over, there is both the start of the next 15 min measurement period and
23
24 411 the start of the processing (5 min, in yellow) + transmission (5 min, in white framed in black) of the one
25
26 412 that has just ended. The measuring periods for an assimilation window [XXXX - 30 min; XXXX + 30 min
27
28 413] would be : XXXX - 37.5 min; XXXX - 22.5 min], [XXXX - 22.5 min; XXXX - 7.5 min], [XXXX - 7.5 min;
29
30 414 XXXX + 7.5 min], [XXXX + 7.5 min; XXXX + 22.5 min], [XXXX + 22.5 min; XXXX + 37.5 min]. So, for a
31
32 415 cut-off time greater than or equal to XXXX + 47.5 min, there are 4 profiles for the corresponding
33
34 416 analysis. The end of the last 5 min transmission window should occur before the so-called cut-off time.
35
36 417 The cut-off time is the time after the hour of analysis until which one waits for the observations to
37
38 418 arrive before starting the calculations. In the current AROME-France assimilation system, this cut-off
39
40 419 is not constant and varies according to the time of day (it varies from T+20 min. to T+3h15). Depending
41
42 420 on the cut-off time, up to 6 WV lidar profiles will be assimilated in each hourly 4DEnVar analysis. This
43
44 421 sequence is subject to adaptation depending on the evolution of the high computational performances
45
46 422 at Météo-France and performances of the WV lidars in the field.

47 423 48 424 ➤ *WV lidars intercomparison*

49 425
50 426 After the conduct of the field campaign, the consortium will also deliver a consistent, self-coherent
51
52 427 and validated WV dataset of lidar profiles, incl. uncertainties at high spatio-temporal resolution for
53
54 428 data assimilation experiments. This effort will include inter-comparison of WV lidar-derived profiles
55
56 429 between the 3 operational systems WALI, BASIL and ARTHUS. Comparison between WALI, LAASURS
57
58 430 and ALIAS will be conducted at LSCE before and after the field campaign. The long-term stability and
59
60 431 calibration of the WV lidar systems will also be monitored throughout the field campaign using a
61
62
63
64
65

432 mobile radiosounding unit that will be operated alongside each of the 6 Raman lidar systems at the
1 433 beginning, mid-way through and at the end of the campaign.

3 434
4
5 435 **WP2 (data monitoring)** aims at Raman lidar data assimilation in AROME-France. This includes
6
7 436 evaluating and optimizing how the observations can be used in the data assimilation system. For this,
8
9 437 the ability of the model to simulate the physical quantity that is observed must be ensured. In practice,
10 438 this is done through the "monitoring" of observations, i.e., the computation of observation-minus-
11
12 439 background statistics, where "background" refers to short-term forecasts that will be blended with
13
14 440 observations during the data assimilation process. Such a monitoring requires some preliminary work.
15
16 441 To compare observations and the background, a common physical space has to be chosen, which
17
18 442 needs to be close to that of the raw measurements to avoid the introduction of retrieval errors, while
19
20 443 lending itself to the simulation from the model prognostic variables. The choice of this physical space
21
22 444 in terms of geometry, physical quantity, and observation processing (time-space averaging, filtering)
23
24 445 will be carefully assessed based on the horizontal and vertical resolutions of the current AROME-France
25
26 446 version (e.g., 1.3 km) and the 15 min period of observations use. The current version of AROME-France
27
28 447 uses a three-dimensional variational (3D-Var) algorithm to assimilate weather data. A four-
29
30 448 dimensional Ensemble-Variational (4DEnVar) data assimilation system will be available in 2022 to
31
32 449 replace the current 3D-Var data assimilation system. It will be used in place of the 3D-Var data
33
34 450 assimilation system for the WaLiNeAs project.

35 451
36 452 A near real-time monitoring will be set up during the field campaign scheduled in the fall of 2022 that
37
38 453 will enable the evaluation of the statistical consistency between the observations and the model
39
40 454 background. Such a real-time monitoring is usually performed at operational weather forecasting
41
42 455 centres to detect gross errors such as hardware failure, calibration drift, or transmission losses. The
43
44 456 monitoring performed in the framework of WaLiNeAs will ensure that the data are collected as
45
46 457 expected and, if needed, allow for corrective action to be taken immediately so as to minimize any
47
48 458 data loss.

49 459
50 460 After the field campaign, observation-minus-background statistics will be performed on the consistent,
51
52 461 self-coherent and validated dataset of lidar profiles, once it is available (**WP1**). The objective is to
53
54 462 compare to which extent the real-time and post-processed lidar data differ with respect to the model.
55
56 463 Depending on the results, observation-minus-background biases will be removed so as to comply with
57
58 464 the data assimilation technique assumptions. The resulting lidar data sets and observation operator
59
60 465 will be used in **WP3** for the data assimilation experiments.

469 **WP3 (lidar data assimilation)** is focused on the post-campaign work on the assessment of the lidar
1 470 data impact in the assimilation scheme. Since the objective of the project is to prove the feasibility and
2 471 benefit of assimilating lidar data in an operational context, the assessment of the impact of the lidar
3 472 data assimilation will be carried out by performing data assimilation experiments with the AROME-
4 473 France system. The proven methodology of Observing System Experiments will be used. It consists in
5 474 running two different experiments: the reference experiment, while the data assimilation experiment
6 475 will additionally assimilate lidar data. So, the reference experiment will already assimilate all routinely
7 476 available observations, and thus the impact of lidar observations will translate the ability of this new
8 477 observing system to complement existing observing systems. With this methodology, the impact of
9 478 the lidar data assimilation is simply obtained by contrasting the weather forecasts obtained by each of
10 479 the two experiments with respect to an independent observational data set (e.g., precipitation
11 480 amounts measured by rain gauges).

12 481
13 482 Data assimilation experiments will be performed for the two data sets prepared in WP1 and WP2: a
14 483 set of lidar data collected in real-time, and a set of consistent, self-coherent and validated lidar data.
15 484 The real-time data set will provide baseline results that will show which benefit can readily be obtained
16 485 with the current real-time data processing. The post-processed data set will show to which extent
17 486 additional processing may improve the quality of the weather forecasts. This will likely lead to
18 487 recommendations on the lidar data processing for future operational exploitation in NWP systems.

19 488
20 489
21 490 **WP4 (HPE related science)** is expected to provide an improved representation of the highly variable
22 491 spatial-temporal distribution of WV in the AROME-France analyses from the advanced data
23 492 assimilation implemented in this project, that will in turn lead to an overall improvement of the
24 493 complex thermodynamical and dynamical processes controlling the life cycle of HPEs. We will
25 494 investigate the impact of the WV profiles processing (real-time Vs validated lidar data) on (i) the WV
26 495 distribution over the western Mediterranean in the AROME-France model, and (ii) the prediction of
27 496 the position, evolution and the rainfall amount of the precipitating systems and HPEs encountered
28 497 during the 3-month field campaign. The results will also be compared to AROME-France reference
29 498 simulations in which lidar-derived WV profiles are not assimilated to further emphasize the worth (or
30 499 lack thereof) of assimilating such data in the French NWP system. In addition, with a similar approach,
31 500 we will examine what is gained in terms of advancing our knowledge of complex processes pertaining
32 501 to the characteristics of the moist inflow (origin, evolution, pathways) feeding deep convection leading
33 502 to HPEs. We will also study the impact of dry intrusions from the upper troposphere and moist tropical
34 503 plumes on HPEs encountered during the campaign.
35 504

505 Outlook

1 506
2 507 This project aims at the development of all-weather, unattended, rugged and operational Raman lidar
3
4 508 systems for smart monitoring of the environment, and WV in particular. The WaLiNeAs project aims at
5
6 509 developing the test bed of an integrated prediction tool, coupling network measurements of WV
7
8 510 profiles and a weather forecast model to precisely estimate precipitable water upstream of an event
9
10 511 up to 48 hours in advance in Southern France. This project is highly innovative and will lay the
11
12 512 foundation for a future integrated warning tool aiming to prevent natural hazards associated with HPEs
13
14 513 as often experienced along the Mediterranean coastline. Once the proof of concept is validated in the
15
16 514 framework of the WaLiNeAs project, similar integrated tools may be applied in other parts of the World
17
18 515 to avoid similar natural hazards.

19 516
20 517 The highest risk for the project lies with the meteorology and the possible lack of heavy precipitation
21
22 518 events during the fall of 2022. However, the length of the field campaign (3 months) is the best
23
24 519 insurance that extreme events will happen somewhere in northwestern Mediterranean. Nevertheless,
25
26 520 on average, ~ 7 HPEs (daily rainfall > 150 mm) occur every year between September and November
27
28 521 (Ricard et al. 2012, Figure 2). Furthermore, even in the case of lower than average HPE activity in
29
30 522 southern France, the network data will be beneficial to the AROME-France forecasts, and a positive
31
32 523 impact is expected on average skill scores and in the case of southern maritime inflow situation.
33
34 524 Furthermore, experience learned from the lidar data processing in near-real time and assimilation in
35
36 525 NWP systems will still be extremely valuable to make recommendation on the use of WV lidars for
37
38 526 future operational NWP systems. In all cases, the uttermost important objective of the project is to
39
40 527 contribute to increase the accuracy of forecasts of quantitative precipitation in order to satisfy the
41
42 528 societal demands in terms of amount, timing, and basin-specific locations of rainfall and flash flooding.

43 529 Acknowledgements

44
45
46 530 The authors would like to thank Evelyne Richard and Mathieu Nuret, now retired, who have
47
48 531 contributed to the original version of the WaLiNeAs proposals submitted to ANR in 2018 and 2019.

50 532 Funding

51
52 533 This work is a follow-on initiative to the HyMeX programme supported by MISTRALS and the Agence
53
54 534 Nationale de la Recherche WaLiNeAs Grant ANR-20-CE04-0001. Additional funding was also obtained
55
56 535 from the H2020 program of the European Union (grant agreement no. 654109, 778349, 871115), the
57
58 536 Spanish Ministry of Science and Innovation (ref. PID2019-103886RB-I00), the Spanish Ministry of

537 Economy, Industry and Competitiveness (ref. CGL2017-90884-REDT), and the Unit of Excellence Maria
538 de Maeztu (ref. MDM-2016-0600) financed by the Spanish Agencia Estatal de Investigación.

539 Conflict of interest

540 On behalf of all authors, the corresponding author states that there is no conflict of interest.

541 References

- 542 Balin, I., I. Serikov, S. Bobrovnikov, V. Simeonov, B. Calpini, Y. Arshinoc, and H. van den Bergh, 2004:
543 Simultaneous measurement of atmospheric temperature, humidity, and aerosol extinction and
544 backscatter coefficients by a combined vibrational–pure-rotational Raman lidar. *Appl Phys B*, 79,
545 775-782.
- 546 Bhawar, R., P. Di Girolamo, D. Summa, C. Flamant, D. Althausen, A. Behrendt, C. Kiemle, P. Bossler, M.
547 Cacciani, C. Champollion, T. Di Iorio, R. Engelmann, C. Herold, S. Pal, M. Wirth and V. Wulfmeyer,
548 2011: The water vapour intercomparison effort in the framework of the Convective and
549 Orographically-Induced Precipitation Study: airborne-to-ground-based and airborne-to-airborne
550 lidar systems, *Q. J. Roy. Meteorol. Soc.*, **137**(S1), 325-345.
- 551 Behrendt, A., S. Pal, F. Aoshima, M. Bender, A. Blyth, U. Corsmeier, J. Cuesta, G. Dick, M. Dorninger, C.
552 Flamant, P. Di Girolamo, T. Gorgas, Y. Huang, N. Kalthoff, S. Khodayar, H. Mannstein, K. Träumner,
553 A. Wieser, and V. Wulfmeyer, 2011: Observation of convection initiation processes with a suite of
554 state-of-the-art research instruments during COPS IOP8b. *Q. J. Roy. Meteorol. Soc.* 137 (S1), 81-
555 100.
- 556 Berhendt, A., V. Wulfmeyer, H.-S. Bauer, T. Schaberl, P. Di Girolamo, D. Summa, C. Kiemle, G. Ehret, D.
557 Whiteman, B. Demoz, E. browell, S. Ismail, R. Ferrare, and J. Wang, 2007a: Intercomparison of water
558 vapor data measured with lidar during IHOP_2002, Part 2: Airborne to airborne systems, *J. Ocean.*
559 *Atmos. Tech.*, **24**, 3-21.
- 560 Berhendt, A., V. Wulfmeyer, C. Kiemle, G. Ehret, C. Flamant, T. Schaberl, H.-S. Bauer, S. Kooi, S. Ismail,
561 R. Ferrare and E. Browell, 2007b: Intercomparison of water vapor data measured with lidar during
562 IHOP_2002, Part 2: Airborne to airborne systems, *J. Ocean. Atmos. Tech.*, **24**, 22-39.
- 563 Bielli, S., M. Grzeschik, E. Richard, C. Flamant, C. Champollion, C. Kiemle, M. Dorninger and P.
564 Brousseau, 2012: Assimilation of water vapour airborne lidar observations: Impact study on the
565 COPS precipitation forecasts, *Q. J. Roy. Meteorol. Soc.*, **138**, 1652-1667
- 566 Brocard, E., R. Philipona, A. Haefele, G. Romanens, A. Mueller, D. Ruffierux, V. Simeonov, and B. Calpini,
567 2013: Raman Lidar for Meteorological Observations, RALMO – Part 2: Validation of water vapor
568 measurements, *Atmos. Meas. Tech.*, 6, 1347-1358. doi: 10.5194/amt-6-1347-2013, 2013.

- 569 Brousseau, P., G. Desroziers, F. Bouttier, and B. Chapnik, 2014: A posteriori diagnostics of the impact
1 of observations on the AROME-France convective-scale data assimilation system. *Q. J. of the Roy.*
2 570
3 571 *Meteoro. Soc.*, **140**(680), 982-994.
- 572 Brousseau P., Seity, Y., Ricard, D., and Léger, J., 2016: Improvement of the forecast of convective
6 activity from the AROME-France system. *Quarterly Journal of the Royal Meteorological Society*,
7 573
8 574 **142**(699), 2231-2243.
- 575 Chazette, P., F. Marnas, J. Totems, and X. Shang, 2014: Comparison of IASI water vapor retrieval with
11 H₂O-Raman lidar in the framework of the Mediterranean HyMeX and ChArMEx programs, *Atmos.*
12 576
13 577 *Chem. Phys.*, **14**, 9583-9596, doi:10.5194/acp-14-9583-2014.
- 578 Chazette, P., C. Flamant, J.-C. Raut, J. Totems and X. Shang, 2016b: Tropical moisture enriched storm
17 tracks over the Mediterranean and their link with intense rainfall in the Cevennes-Vivarais area
18 579
19 580 during HyMeX, *Q. J. Roy. Meteorol. Soc.*, **142**, S1, 320–334, doi: 10.1002/qj.2674.
- 581 Chazette, P., C. Flamant, X. Shang, J. Totems, J.-C. Raut, A. Doerenbecher, V. Ducrocq, N. Fourrié, O.
22 Bock, A. Dorenbecher and S. Cloché, 2016a: Multi-instrument and multi-model assessment of
23 582
24 583 atmospheric moisture variability over the Western Mediterranean during HyMeX, *Q. J. Roy.*
25 584
26 584 *Meteorol. Soc.*, **142**, S1, 7–22, doi: 10.1002/qj.2671.
- 585 Chazette, P., J. Totems, A. Baron, C. Flamant, S. Bony, 2020: Trade-wind clouds and aerosols
29 characterized by airborne horizontal lidar measurements during the EUREC⁴A field campaign, *Earth*
30 586
31 587 *Syst. Sci. Data, Earth Syst. Sci. Data*, **12**, 2919–2936.
- 588 Chazette, P., C. Flamant, H. Sodemann, J. Totems, A. Monod, E. Dieudonné, A. Baron, A. Seidl, H.-C.
34 Steen-Larsen, P. Doira, A. Durand, and S. Ravier, 2020: The lacustrine-water vapor isotope inventory
35 589
36 590 experiment L-WAIVE, *Atmos. Chem. Phys. Discuss.*
- 591 Caumont, O., Mandement, M., Bouttier, F., Eeckman, J., Lebeau-pin Brossier, C., Lovat, A., Nuissier, O.,
40 and Laurantin, O., 2020: The heavy precipitation event of 14–15 October 2018 in the Aude
41 592
42 593 catchment: A meteorological study based on operational numerical weather prediction systems
43 594
44 594 and standard and personal observations, *Nat. Hazards Earth Syst. Sci. Discuss.* [preprint],
45 595
46 595 <https://doi.org/10.5194/nhess-2020-310>, in review.
- 596 Desroziers, G., Camino, J.-T. and Berre, L., 2014: 4DEnVar: link with 4D state formulation of variational
49 assimilation and different possible implementations. *Q.J.R. Meteorol. Soc.*, **140**: 2097-2110.
50 597
51 598 doi:[10.1002/qj.2325](https://doi.org/10.1002/qj.2325)
- 599 Di Girolamo, P., B. De Rosa, C. Flamant, D. Summa, O. Bousquet, P. Chazette, J. Totems and M. Cacciani,
54 600
55 600 2020: Water vapour mixing ratio and temperature intercomparison results in the framework of the
56 601
57 601 hydrological cycle in the Mediterranean experiment – special observation period 1, *Bull. Atmos. Sci.*
58 602
59 602 *Tech.*, **1**, 133-153.

603 Di Girolamo, P., M. Cacciani, D. Summa, A. Scoccione, B. De Rosa, A. Behrendt, V. Wulfmeyer, 2017:
1 604 Characterisation of Boundary Layer Turbulent Processes by the Raman Lidar BASIL in the frame of
2 605 HD(CP)2 Observational Prototype Experiment, *Atmospheric Chemistry and Physics*, **17**, 745-767,
3 606 doi:10.5194/acp-17-745-2017.
4
5 607 Di Girolamo, P., C. Flamant, M. Cacciani, E. Richard, V. Ducrocq, D. Summa, D. Stelitano, N. Fourrié and
6 608 F. Saïd, 2016: Observation of low-level wind reversals over the Gulf of Lion and their impact on the
7 609 water vapour variability, *Q. J. Roy. Meteorol. Soc.*, **142**, S1, 153–172, doi: 10.1002/qj.2767.
8
9 610 Di Girolamo, P., D. Summa, D. Sabatino, R. Ferretti and C. Faccani, 2009: Multiparameter Raman Lidar
10 611 Measurements for the Characterization of a Dry Stratospheric Intrusion Event. *Journal of*
11 612 *Atmospheric and Oceanic Technology*, vol. 26, p. 1742-1762, ISSN: 0739-0572, doi:
12 613 10.1175/2009JTECHA1253.1.
13
14 614 Dinoev, T., V. B. Simeonov, Y. Arshinov, S. Bobrovnikov, P. Ristori, B. Calpini, M. Parlange, and H. van
15 615 den Bergh, 2013: Raman Lidar for meteorological observations, RALMO. Part 1: Instrument
16 616 description. *Atmos. Meas. Tech.*, **6**, 1329–1346.
17
18 617 Ducrocq, V., Nuissier, O., Ricard, D., Lebeaupin, C., and Thouvenin, T.: A numerical study of three
19 618 catastrophic precipitating events over southern France. II: Mesoscale triggering and stationarity
20 619 factors, *Quarterly Journal of the Royal Meteorological Society*, **134**, 131–145,
21 620 <https://doi.org/10.1002/qj.199>, 2008.
22
23 621 Ducrocq, V. and co-authors, 2014: HyMeX-SOP1, the field campaign dedicated to heavy precipitation
24 622 and flash flooding in the northwestern Mediterranean, *Bull. Am. Meteor. Soc.*, **95**, 1083–1100.
25
26 623 Duffourg, F., O. Nuissier, V. Ducrocq, C. Flamant, P. Chazette, J. Delanoë, A. Doerenbecher, N. Fourrié,
27 624 P. Di Girolamo, C. Lac, D. Legain, M. Martinet, F. Saïd and O. Bock, 2016: Offshore deep convection
28 625 initiation and maintenance during HyMeX IOP 16a heavy precipitation event, *Q. J. Roy. Meteorol.*
29 626 *Soc.*, **142**, S1, 259–274, doi: 10.1002/qj.2725.
30
31 627 Duffourg, F., K.-O. Lee, V. Ducrocq, C. Flamant, P. Chazette, and P. Di Girolamo, 2018: Role of moisture
32 628 patterns in the backbuilding formation of HyMeX IOP13 Heavy Precipitating Systems, *Q. J. Roy.*
33 629 *Meteorol. Soc.*, **144**, 291-303.
34
35 630 Duffourg, F., V. Ducrocq, 2013: Assessment of the water supply to Mediterranean heavy precipitation :
36 631 a method based on finely designed water budgets. *Atmospheric Science Letters*, **14**(3), 133–138.
37
38 632 Fourrié, N., Nuret, M., Brousseau, P., and Caumont, O., 2021: Data assimilation impact studies with the
39 633 AROME-WMED reanalysis of the first special observation period of the Hydrological cycle in the
40 634 Mediterranean Experiment, *Nat. Hazards Earth Syst. Sci.*, **21**, 463–480,
41 635 <https://doi.org/10.5194/nhess-21-463-2021>.
42
43 636 Fourrié, N., M. Nuret, P. Brousseau, O. Caumont, A. Doerenbecher, E. Wattrelot, P. Moll, H. Bénichou,
44 637 D. Puech, O. Bock, O. Bossler, P. Chazette, C. Flamant, P. Di Girolamo, E. Richard, and F. Saïd, 2019:

638 The AROME-WMED reanalyses of the first Special Observation Period of the Hydrological cycle in
1 639 the Mediterranean experiment, *Geophys. Model Dev.* , 12, 2657–2678.

3 640 Fourrié, N., Bresson, É., Nuret, M., Jany, C., Brousseau, P., Doerenbecher, A., Kreitz, M., Nuissier, O.,
4 641 Sevault, E., Bénichou, H., Amodei, M., and Poupponneau, F, 2015: AROME-WMED, a real-time
5 642 mesoscale model designed for the HyMeX special observation periods, *Geosci. Model Dev.*, 8, 1919-
6 643 1941.

10 644 Gaume, E. and co-authors, 2009: A compilation of data on European flash floods. *J. Hydrol.*, **367**, 70–
11 645 78.

14 646 Grzeschik, M., H.-S. Bauer, V. Wulfmeyer , D. Engelbart, U. Wandinger, I. Mattis, D. Althausen, R.
15 647 Engelmann, M. Tesche, and A. Riede, 2008. Four dimensional variational data analysis of water
16 648 vapor Raman lidar data and their impact on mesoscale forecasts. *J. Atmos. Ocean. Technol.* **25**: 1437–
17 649 1453.

21 650 Goldsmith, J. E., Forest H. Blair, Scott E. Bisson, and David D. Turner, 1998: Turn-key Raman lidar for
22 651 profiling atmospheric water vapor, clouds, and aerosols, *Appl. Opt.* 37, 4979-4990.

24 652 Gustafsson, N., T. Janjić, C. Schraff, D. Leuenberger, M. Weissmann, H. Reich, P. Brousseau, T.
25 653 Montmerle, E. Wattrelot, A. Bučánek, M. Mile, R. Hamdi, M. Lindskog, J. Barkmeijer, M. Dahlbom,
26 654 B. Macpherson, S. Ballard, G. Inverarity, J. Carley, C. Alexander, D. Dowell, S. Liu, Y. Ikuta, T. Fujita,
27 655 2018: Survey of data assimilation methods for convective-scale numerical weather prediction at
28 656 operational centres. *Q. J. R. Meteorol. Soc.* doi:[10.1002/qj.3179](https://doi.org/10.1002/qj.3179)

33 657 Khodayar, S., B. Czajka, A. Caldas-Alvarez, S. Helgert, C. Flamant, P. *Di Girolamo*, O. Bock and P.
34 658 Chazette, 2018: Multi-scale Observations of Moisture Feeding Heavy Precipitating Systems in the
35 659 Northwestern Mediterranean during HyMeX IOP12, *Q. J. Roy. Meteorol. Soc.*, 2761-2780.

38 660 Kwon I.-H., S. English, W. Bell, R. Potthast, A. Collard, and B. Ruston, 2018: Assessment of progress and
39 661 status of data assimilation in numerical weather prediction, *Bull. Amer. Meteorol. Soc.*, **98**, ES75-
40 662 ES79.

44 663 Lange, D., Behrendt, A., & Wulfmeyer, V., 2019: Compact operational tropospheric water vapor and
45 664 temperature Raman lidar with turbulence resolution. *Geophysical Research Letters*, 46, 14,844–
46 665 14,853, <https://doi.org/10.1029/2019GL085774>

49 666 Lenschow, D. H., V. Wulfmeyer, and C. Senff, 2000: Measuring second-through fourth-order moments
50 667 in noisy data. *J. Atmos. Oceanic Technol.* 17 (10), 1330-1347.

53 668 Leuenberger, D., A. Haeferle, N. Omanovic, M. Fengler, G. Martucci, B. Calpini, O. Fuhrer, and A. Rossa,
54 669 2020: Improving High-Impact Numerical Weather Prediction with Lidar and Drone Observations,
55 670 *Bull. Amer. Meteorol. Soc.*, **101**, 1036-1051, <https://doi.org/10.1175/BAMS-D-19-0119.1>.

- 671 Llasat, C., M. Llasat-Botija, O. Petrucci, A. A. Pasqua, J. Rosselló, F. Vinet, and L. Boissier, 2013: Towards
1 672 a database on societal impact of Mediterranean floods within the framework of the HYMEX project.
2
3 673 *Nat. Hazards Earth Syst. Sci.*, **13**, 1337–1350.
4
- 5 674 Montmerle, T, Y. Michel, E. Arbogast, B. Ménétrier, and P. Brousseau, 2018: A 3D ensemble variational
6
7 675 data assimilation scheme for the limited-area AROME model: Formulation and preliminary results.
8
9 676 *Q J R Meteorol Soc.*, 144: 2196– 2215. <https://doi.org/10.1002/qj.3334>
- 10 677 Reichardt, J., U. Wandinger, V. Klein, I. Mattis, B. Hilber, and R. Begbie, 2012: RAMSES: German
11
12 678 Meteorological Service autonomous Raman lidar for water vapor, temperature, aerosol, and cloud
13
14 679 measurements. *Appl. Opt.*, **51**, 8111–8131.
- 15 680 Muñoz-Porcar, C., M. Sicard, M. J. Granados-Muñoz, R. Barragán, A. Comerón, F. Rocadenbosh, A.
16
17 681 Rodríguez-Gómez, and D. Garcia-Vizcaino, 2021: Synergy of Raman Lidar and Modeled Temperature
18
19 682 for Relative Humidity Profiling: Assessment and Uncertainty Analysis, *IEEE Trans. Geosci. Remote*
20
21 683 *Sens.*, **59**, 1-12.
- 22 684 Muñoz-Porcar, C., A. Comerón, M. Sicard, R. Barragán, D. Garcia-Vizcaino, A. Rodríguez-Gómez, F.
23
24 685 Rocadenbosh, and M. J. Granados-Muñoz, 2018: Calibration of Raman lidar water vapor mixing
25
26 686 ratio measurements using zenithal measurements of diffuse sunlight and a radiative transfer
27
28 687 model, *IEEE Trans. Geosci. Remote Sens.*, 56, 7405–7414.
- 29 688 Nuissier, O., Ducrocq, V., Ricard, D., Lebeaupin, C., and Anquetin, S.: A numerical study of three
30
31 689 catastrophic precipitating events over southern France. I: Numerical framework and synoptic
32
33 690 ingredients, *Quarterly Journal of the Royal Meteorological Society*, 134, 111–130,
34
35 691 <https://doi.org/10.1002/qj.200>, 2008.
- 36 692 Ribes, A., S. Thao, R. Vautard, B. Dubuisson, S. Somot, J. Colin, S. Planton and J.-M. Soubeyroux, 2019:
37
38 693 Observed increase in extreme daily rainfall in the French Mediterranean. *Clim. Dyn.*, 52, 1095-1114,
39
40 694 [10.1007/s00382-018-4179-2](https://doi.org/10.1007/s00382-018-4179-2).
- 41 695 Ricard, D. V. Ducrocq, and L. Auger, 2012: A climatology of the mesoscale environment associated with
42
43 696 heavily precipitating events over a northwestern Mediterranean area. *J. Appl. Meteor. Climatol.*,
44
45 697 **51**, 468–488.
- 46 698 Richard E. and co-authors, 2014: Assimilation of LEANDRE II water observations: impact study on the
47
48 699 HyMeX SOP1 precipitation forecasts, 8th HYMEX Workshop, Valletta, Malta, 15-18 September 2014.
- 49 700 Seity Y., P. Brousseau, S. Malardel, G. Hello, P. Bénard, F. Bouttier, C. Lac, and V. Masson, 2011: The
50
51 701 AROME-France convective scale operational model. *Mon. Weather Rev.* **139**: 976–991.
- 52 702 Stelitano, D., P. Di Girolamo, A. Scoccione, D. Summa, and M. Cacciani, 2019: Characterization of
53
54 703 atmospheric aerosol optical properties based on the combined use of a ground-based Raman lidar
55
56 704 and an airborne optical particle counter in the framework of the Hydrological Cycle in the
57
58
59
60
61
62
63
64
65

705 Mediterranean Experiment – Special Observation Period 1, *Atmos. Meas. Tech.*, 12, 2183–2199,
1 706 doi: 10.5194/amt-12-2183-2019.
2
3 707 Stevens, B. and co-authors, 2021: EUREC⁴A, *Earth Syst. Sci. Data.*, *submitted*.
4
5 708 Thundathil, R., T. Schwitalla, A. Behrendt, S. K. Muppa, S. Adam, and V. Wulfmeyer, 2020: Assimilation
6
7 709 of lidar water vapour mixing ratio and temperature profiles into a convection-permitting model. *J.*
8
9 710 *Meteorol. Soc. Japan* 98.
10 711 Totems, J., P. Chazette, and J.-C. Raut, J., 2019: Accuracy of current Arctic springtime water vapour
11
12 712 estimates, assessed by Raman lidar. *Quarterly Journal of the Royal Meteorological Society*,
13
14 713 145(720), 1234–1249. <https://doi.org/10.1002/qj.3492>.
15
16 714 Weckwerth T., D. Parsons, S. Koch, J. Moore, P. Lemone, B. Demoz, C. Flamant, B. Geerts, J. Wang and
17
18 715 W. Feltz, 2004: An Overview of the International H2O Project (IHOP_2002) and Some Preliminary
19
20 716 Highlights, *Bull. Amer. Meteorol. Soc.*, **85**, 253-277.
21 717 Wulfmeyer, V., R. M. Hardesty, D. D. Turner, A. Behrendt, M. P. Cadetdu, P. Di Girolamo, P. Schlüssel,
22
23 718 J. Van Baelen, and F. Zus, 2015: A review of the remote sensing of lower tropospheric
24
25 719 thermodynamic profiles and its indispensable role for the understanding and the simulation of
26
27 720 water and energy cycles, *Rev. Geophys.*, 53, 819–895.
28 721 Wulfmeyer V., H.-S. Bauer, M. Grzeschik, A. Behrendt, F. Vandenberghe, E. V. Browell, S. Ismail, and R.
29
30 722 A. Ferrare, 2006. Four-dimensional variational assimilation of water vapor differential absorption
31
32 723 lidar data: The first case study within IHOP-2002. *Mon. Weather Rev.* **134**: 209–230.
33 724 Yoshida, S., S. Yokota, H. Seko, T. Sakai, and T. Nagai, 2020: Observation system simulation
34
35 725 experiments of water vapor profiles observed by Raman lidar using LETKF system. *SOLA*, 16,
36
37 726 43–50, doi:10.2151/sola.2020-008.
38
39 727
40 728

16
17
18
19
20
21
22
23
24
25
26
27
28
29
30
31
32
33
34
35
36
37
38
39
40
41
42
43
44
45
46
47
48
49
50
51
52
53
54
55
56
57
58
59
60
61
62
63
64
65

Tables

	WALI	ARTHUS	BASIL	UPC/EARLINET
Laser	Nd:YAG	Nd:YAG	Nd:Yag	Nd:Yag
Pulse Energy and initial wavelength	60 mJ at 355 nm	100 mJ at 355 nm	500 mJ at 355 nm 300 mJ at 532 nm 400 mJ at 1064 nm	60 mJ at 355 nm 130 mJ at 532 nm 130 mJ at 1064 nm
Frequency	20 Hz	200 Hz	20 Hz	20 Hz
Reception channels	Elastic total 354.67 nm Elastic \perp 354.67 nm Raman N ₂ 386.63 nm Raman H ₂ O 407.5 nm Elastic \perp 354.67 nm Roto-vib. Raman N ₂ 386.63 nm Roto-vib. Raman H ₂ O 407.5 nm Rotot. Raman (N ₂ &O ₂) - Low J 354.3 nm Rotot. Raman (N ₂ &O ₂) - High J 352.9 nm	Elastic, 355 nm Rot. Ram. 1, CWL selectable Rot. Ram. 2, CWL selectable Raman H ₂ O, 408 nm	Elastic total 354.67 nm Elastic \parallel 354.67 nm Elastic \perp 354.67 nm Elastic total 532.05 nm Elastic \parallel 532.05 nm Elastic total 1064.1 nm Roto-vib. Raman N ₂ 386.63 nm Roto-vib. Raman H ₂ O 407.5 nm Roto-vib. Raman N ₂ 607.4 nm Roto-vib. Raman N ₂ 607.4 nm Rotot. Raman (N ₂ &O ₂) - Low J 354.3 nm Rotot. Raman (N ₂ &O ₂) - High J 352.9 nm	Elastic total 354.7 nm Elastic \perp 354.7 nm Elastic total 532.1 nm Elastic \perp 532.1 nm Elastic total 1064.1 nm Rot. Raman (N ₂ &O ₂) 353.9 nm Rot.-vib. Raman H ₂ O 407.5 nm Rot. Raman (N ₂ &O ₂) 530.2 nm
Receiver diameter	~15 cm	~40 cm	45 cm	40 cm
Field of view	~ 2.3 mrad	< 1 mrad	0.45 mrad (FWHM)	1.2 mrad
Lowest useful range bin	~ 300 m	~ 50 m	~ 500 m (~ 100 for 532.05 nm total & \parallel and 1064.1 nm total)	~ 400 m after overlap correction
Detector	Photomultiplier tubes	Photomultiplier tubes	Photomultiplier tubes	Photomultiplier tubes
Filter bandwidths	0.2–0.3 nm	0.3–0.5 nm	0.2–1.0 nm	0.8–1.0 nm
Vertical sampling	0.75 m (analog) 15 m (photon counting)	7.5 m (analog) 7.5 m (photon counting)	7.5 m (analog & photon counting)	3.75 m (analog & photon counting)
Vertical resolution	~ 30 m	~ 30 m	7.5-150 m	≥ 3.75 m (adjustable)
Acquisition system	PXI technology at 200 MHz	LICEL GmbH	Licel at 200 MHz, FastComTec at 250 Mhz	LICEL GmbH

15
16
17
18
19
20
21
22
23
24
25
26
27
28
29
30
31
32
33
34
35
36
37
38
39
40
41
42
43
44
45
46
47
48
49
50
51
52
53
54
55
56
57
58
59
60
61
62
63
64
65

Table 1: Main technical characteristics of the lidar instruments

1
2
3
4
5
6
7
8
9
10
11
12
13
14
15
16
17
18
19
20
21
22
23
24
25
26
27
28
29
30
31
32
33
34
35
36
37
38
39
40
41
42
43
44
45
46
47
48
49
50
51
52
53
54
55
56
57
58
59
60
61
62
63
64
65

Figures

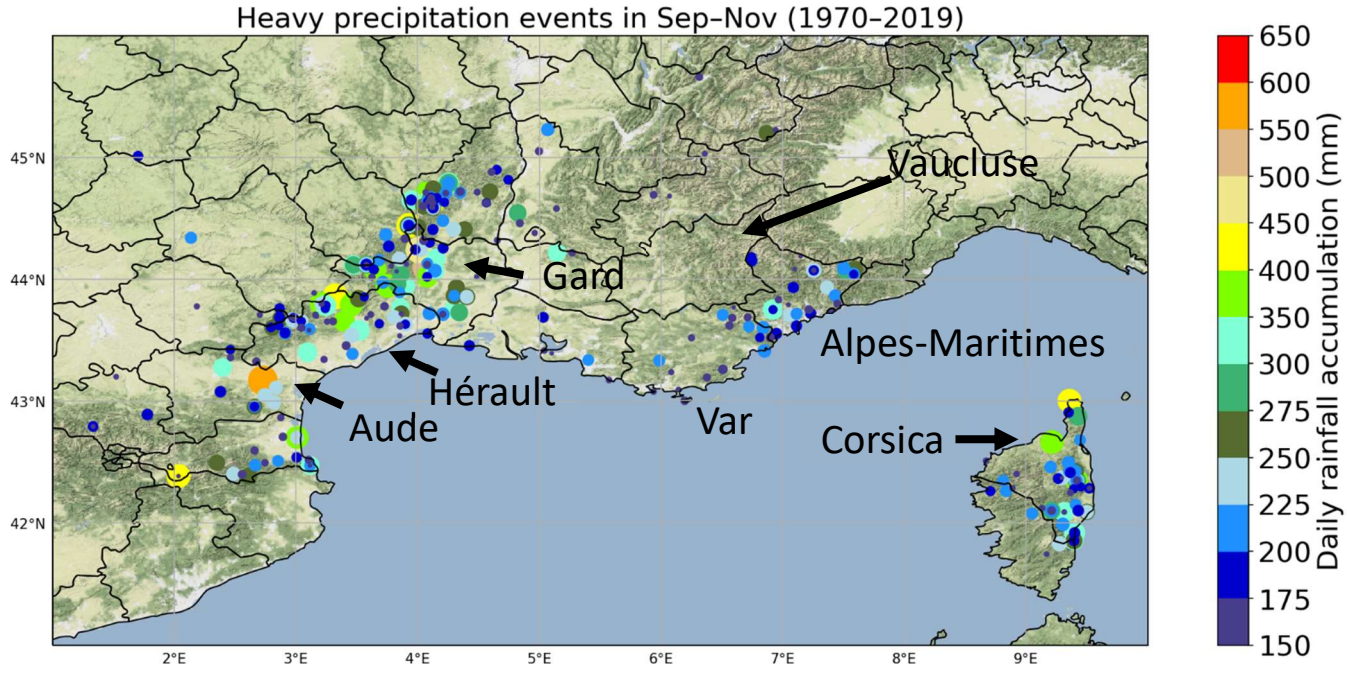


Figure 1: Geographical distribution of heavy precipitation events defined as maximum accumulation > 150 mm/day and separated from other events by a distance of more 100 km.

Heavy precipitation events (1970-2019)

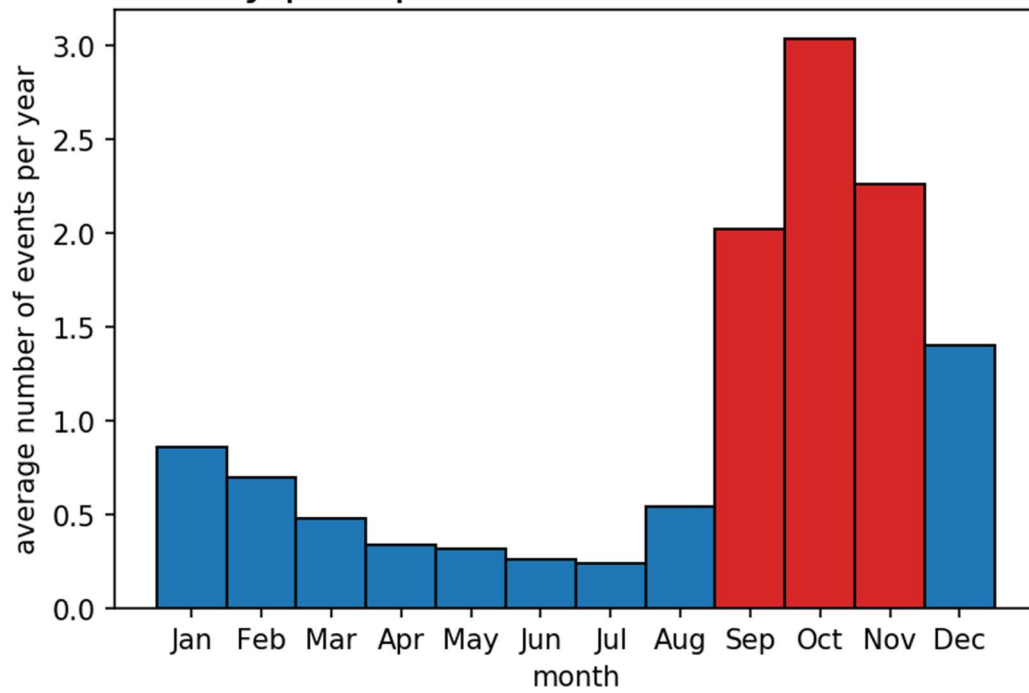


Figure 2: Frequency of monthly heavy precipitation events per year averaged over the period 1970-2019, highlighting in red the three most likely months (September-October-November).

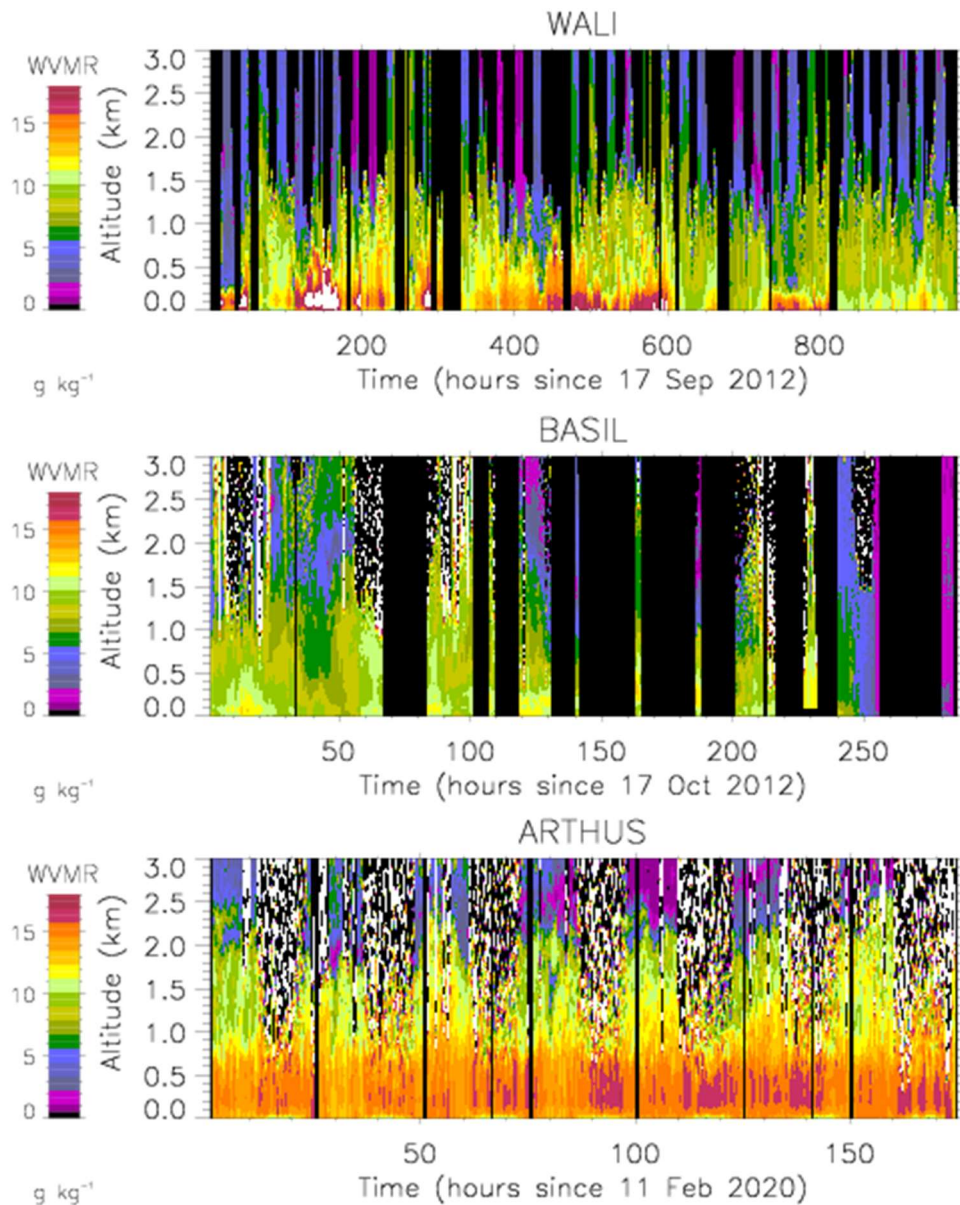


Figure 3: (a) Time-height cross-section of water vapor mixing ratio acquired during the HyMeX SOP1 with the WALI system of LSCE (~1000 h of data) from 17 September to 28 October 2012 over Menorca. The temporal resolution is 1 h and a gliding average of 15 m was applied in the vertical. (b) Same as (a) but measured by BASIL over the 12-day time period from 0000 UTC on 17 October 2012 to 0000 UTC on 27 October 2012 during HyMeX. The temporal resolution is 5 min and a gliding average of 150 m was applied in the vertical. (c) same as (a) measured by ARTHUS collected between 11 and 19 February 2020 onboard the research vessel Maria S. Merian within the EUREC4A deployment. The temporal resolution is 10 s and a gliding average of 50 m was applied in the vertical. The black/white areas correspond to missing data due to the limitation of the detection system during the daytime. The black areas correspond to missing data due to the limitation of the detection system during the daytime or lidar system operation stoppage.

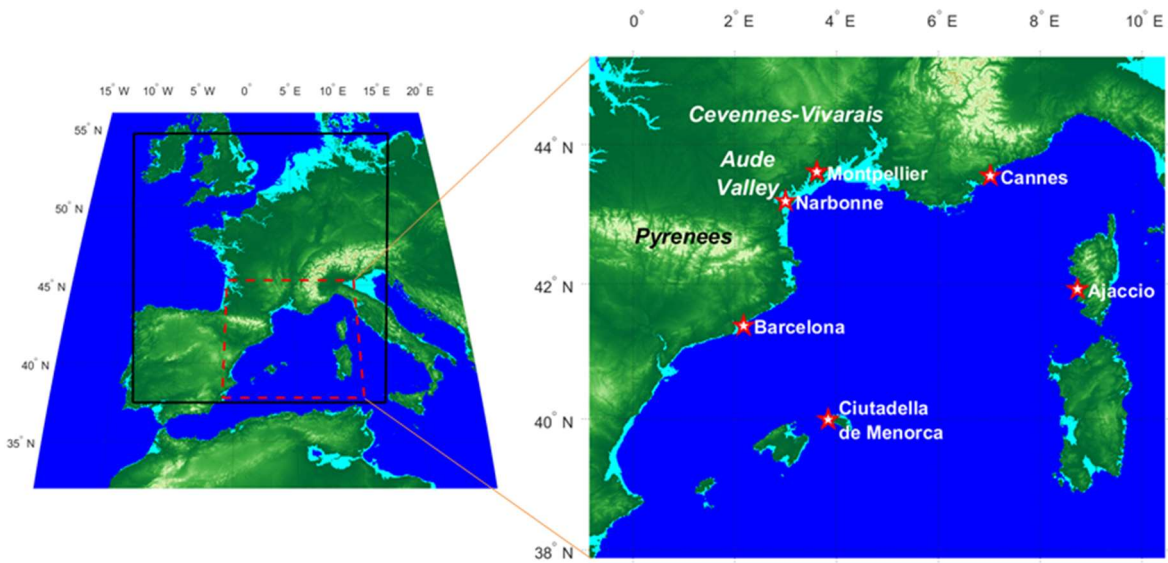


Figure 4: Left: Orography of the AROME-France domain (area delimited by the back contour). Right: zoom on the region of operation of the Raman Lidar Network with the location (city) of each lidar highlighted with red & white stars.

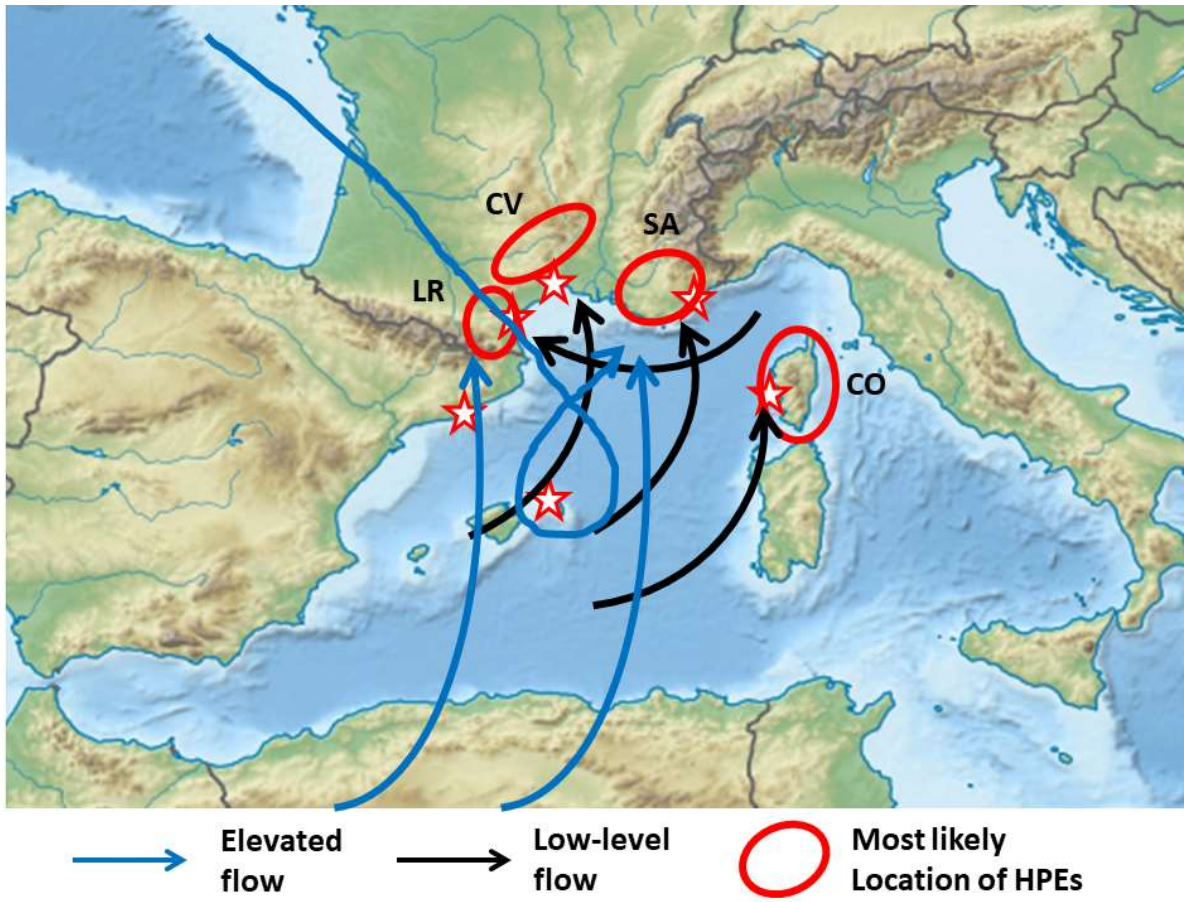


Figure 5: Regions most likely to be impacted by HPEs (red circles) together with main flow patterns in the low-levels (black arrows) and in altitude (2-4 km, blue arrows). LR is Languedoc-Roussillon, CV is Cévennes-Vivarais, SA is southern Alps and CO is Corsica.

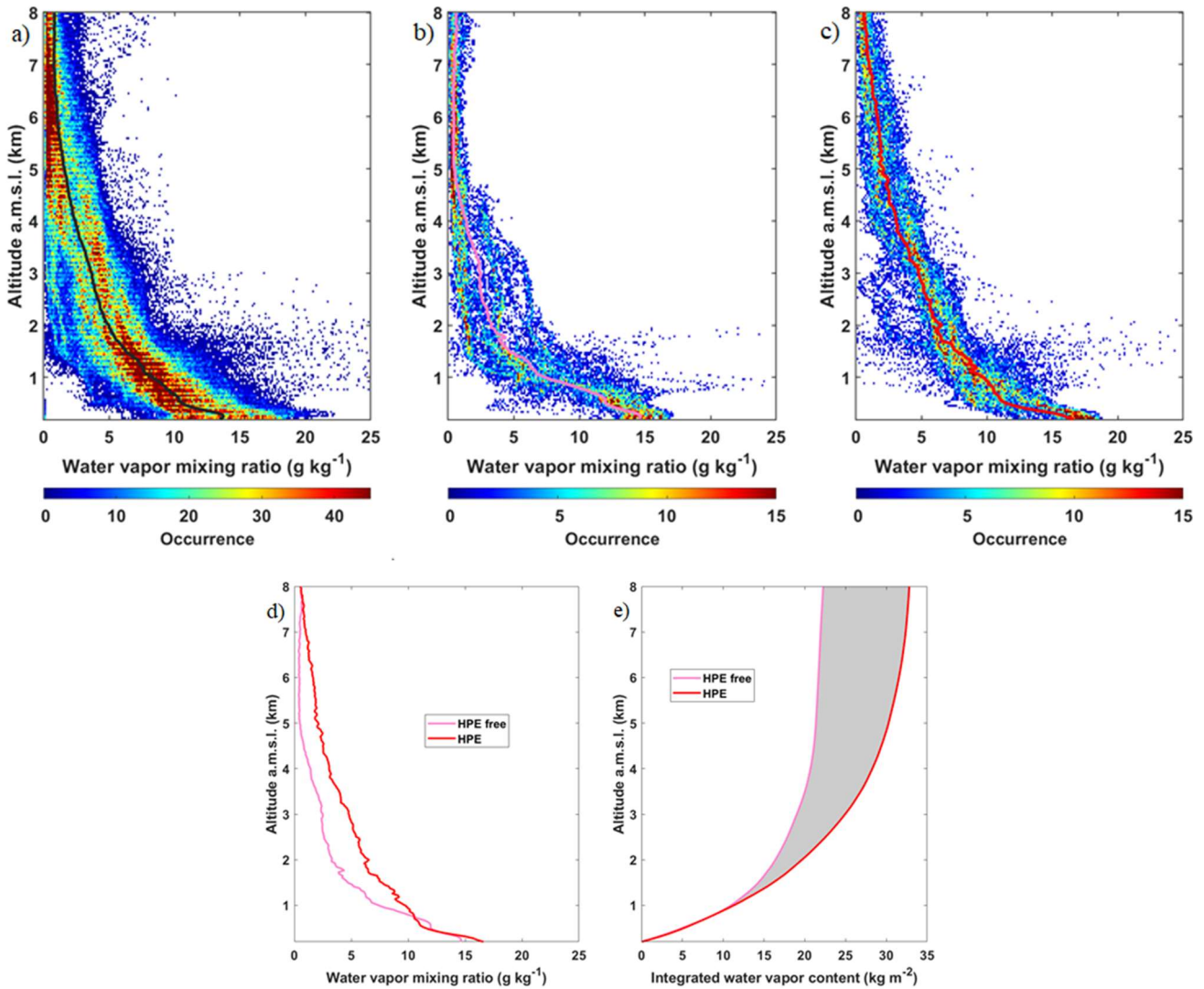


Figure 6: (a) Density distribution of all WV vertical profiles acquired with WALI during the HyMeX SOP1 (see Figure 5a). The black solid line indicate the barycenter of the distribution at each altitude bin. The occurrence of water vapor mixing ratio values is color code. (b) Same as (a), but for the profiles acquired in HPE-free conditions from 2 to 6 October 2012. The pink solid line indicate the barycenter of the distribution at each altitude bin. (c) Same as (b), profiles acquired in HPE conditions from 7 to 11 October 2012. The red solid line indicate the barycenter of the distribution at each altitude bin. (d) Average vertical distribution of WV mixing ratio as a function of altitude in the HPE-free case (pink solid line) and the HPE case (red solid line). (e) Integrated water vapour content as a function of altitude for the HPE-free case (pink solid line) and the HPE case (red solid line). The integrated content is computed at the integral of the lidar-derived specific humidity profiles from the ground upward. The shaded area highlights the difference between the HPE-free and HPE distribution.

1
2
3
4
5
6
7
8
9
10
11
12
13
14
15
16
17
18
19
20
21
22
23
24
25
26
27
28
29
30
31
32
33
34
35
36
37
38
39
40
41
42
43
44
45
46
47
48
49
50
51
52
53
54
55
56
57
58
59
60
61
62
63
64
65

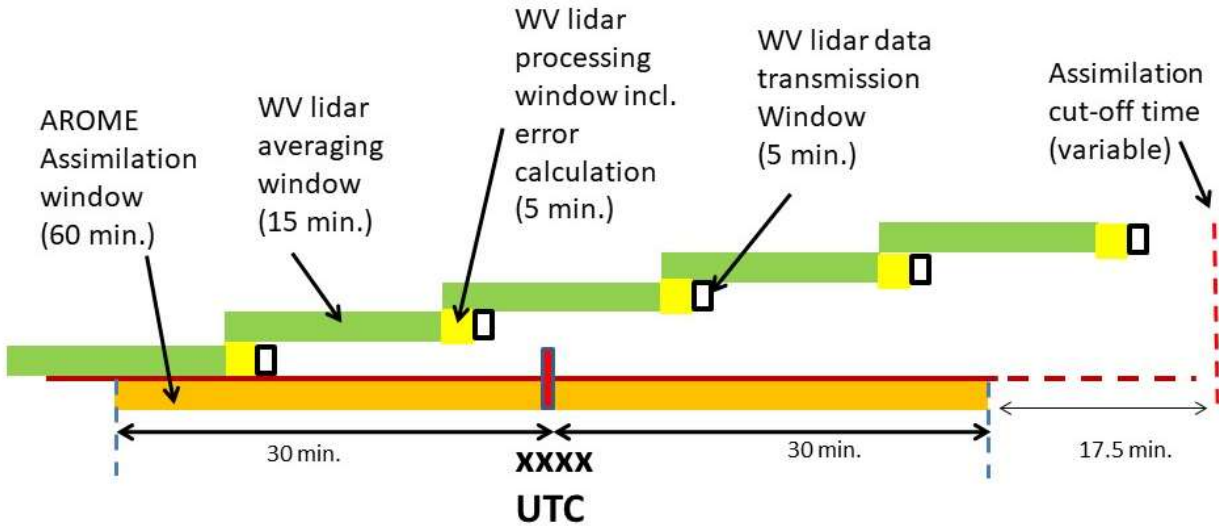


Figure 7: Timeline of the WV lidar data transmission sequence from the operating sites to Météo-France for assimilation of near-real time WV profiles in the AROME-France NWP system.